Mantle wedge serpentinization and exhumation of eclogites: Insights from eastern Ladakh, northwest Himalaya

Stéphane Guillot Centre National de la Recherche Scientifique, Université de Lyon I, 69622 Villeurbanne, France
Kéiko H. Hattori Department of Earth Sciences, University of Ottawa, Ottawa, Ontario K1N 6N5, Canada
Julia de Sigoyer Institut de Géologie, Universite de Neuchâtel, CH-2007 Neuchâtel, Switzerland

ABSTRACT

In eastern Ladakh, northwest Himalaya, serpentinite layers occur in close association with eclogites. The occurrence of metamorphic olivine and talc in serpentinites suggests that the serpentinization and eclogitization took place under similar conditions (600 °C, 20 kbar). The serpentinites and eclogites show similar deformation, including the direction of normal shearing. The highly refractory nature of the serpentinite protolith, as shown by the composition of bulk rocks and chromite and the concentrations of Re and platinum group elements, indicates their derivation from mantle wedge. We propose that the serpentinites formed by hydration of the mantle wedge as a result of dewatering of the subducted slab. The serpentinites then facilitated exhumation of the subducted rocks by acting as a lubricant. At shallow depths, sediments are generally considered to be the lubricant for the exhumation, but serpentinites may commonly take over this role at greater depths. Under sediment-poor conditions, serpentinites may contribute to the exhumation even at shallower depths. This may explain the close spatial association of serpentinites and partially hydrated peridotites with many well-known high-pressure to ultrahigh-pressure metamorphic belts worldwide.

Keywords: serpentinite, PGE, platinum group elements, ultrahigh pressure, exhumation, subduction, Himalaya.

INTRODUCTION

Various processes have been proposed to explain the exhumation of blueschist and eclogitic rocks (Platt, 1993), and the upward flow of rocks in an accretionary wedge is most commonly advocated (Cloos and Shreve, 1988; Allemand and Lardeaux, 1997). However, this process requires lubricating layers in exhumation zones. Hydrated sediments in accretionary wedges may act as a lubricant for the exhumation of high-pressure (P <20 kbar; <500 °C) rocks (Cloos and Shreve, 1988). At greater depths, sediments are less abundant and would not play the role as a lubricant for the exhumation of ultrahigh-P (>20 kbar, >500 °C) rocks. Serpentinites and partially hydrated peridotites are spatially associated with many ultrahigh-P rocks (Table 1), suggesting the possible role of serpentinites in the exhumation of ultrahigh-P rocks. To evaluate this possibility, we collected serpentinites intimately associated with the ultrahigh-P Tso Morari unit in eastern Ladakh in the northwest Himalaya. For comparison, we also collected serpentinites from different units of the Indus suture zone.

TABLE 1. ULTRAHIGH-PRESSURE AND HYDRATED PERIDOTITES

Locality	Structural association
Saas-Fee, Alps*	Inside pods and bounding fault
Voltri massif, Alps†	Inside pods and bounding fault
Dabie Shan, China§	Inside pods
Central Indonesia#	Bounding fault
Kokchetav, Kazakhstan**	Inside pods
Lepontine, Alps††	Macroboudin
Ronda massif, Spain††	Macroboudin
Massif Central, France††	Inside pods
Caledonides, Norway††	Inside pods
Bohemian massif, Czech††	Inside pods and bounding fault
Erzgebirge, Germany§§	Inside pods

*Barnicoat and Fry (1986).
†Scambelluri et al. (1995).
§Zhang and Liou (1994).
#Parkinson et al. (1997).
**Maruyama et al. (1997).
††Medaris and Carswell (1990).
§§Schmädicke et al. (1992).

Petrogenetic studies of serpentinites are difficult because their primary minerals are commonly obliterated. They also contain very low concentrations of incompatible elements, which are useful for petrogenetic studies, and their compositions can easily be modified during their hydration. Serpentinites, however, contain high concentrations of platinum group elements (PGEs). We report the concentration of PGEs and the composition of chromite to evaluate the origin of serpentinites and to assess their possible role in the exhumation of eclogites. Our findings may have relevance to many orogenic metamorphic belts where serpentinites are commonly associated with ultrahigh-P rocks.

GEOLOGIC SETTING

The Ladakh area is considered to be a subduction complex that was active from the middle Cretaceous to the late Paleocene (Honegger et al., 1982). The Ladakh calc-alkaline batholith, the Indus suture zone, and the Tso Morari unit are exposed from north to south (Fig. 1). The suture zone consists of the Tertiary Indus clastic sedimentary rocks, the Nidar arc complex, and a tectonic melange, the latter containing continental sedimentary rocks and volcanic rocks of oceanic island origin (the Drakkarpo and Ribil units; de Sigoyer, 1998). The suture zone is separated from the eclogitic Tso Morari unit by the Zildat normal fault, along which serpentinite layers ~100 m thick are boudinaged to discontinuous lenses, 100 × 1000 m in size. The Tso Morari unit is a 100 × 50 km block of ultrahigh-P rocks formed from Indian continental margin during its subduction in the late Paleocene (de Sigoyer, 1998). The serpentinites on the northern margin of the Tso Morari unit are intensely deformed, and the style of deformation, including top-to-

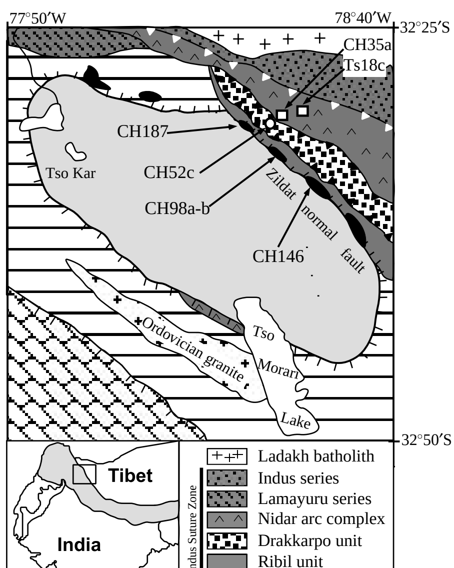

Figure 1. Geologic map of eastern Ladakh, northwest Himalaya, showing occurrence of ultrahigh-pressure Tso Morari unit and serpentinites. Sample locations are shown with arrows. Inset key corresponds to Himalaya-Karakoram belt. Serpentinite layers occur discontinuously along northern boundary of Tso Morari unit. Intense shearing resulted in boudinage of serpentinites. Samples were collected from thickened portions of serpentinite layers.

Data Repository item 200022 contains additional material related to this article.

the-northeast normal shearing, is identical to that in the Tso Morari unit (Fig. 1).

SAMPLING AND ANALYTICAL METHODS

The samples TS18c and CH35a come from the lower part of the Nidar ophiolite (Fig. 1). Sample CH52C is from the Drakkarpo unit. Samples CH98a, CH98b, CH146, and CH187 are from the Zildat normal fault, which is in contact with the Tso Morari eclogites. Major and minor element concentrations were determined using Philips PW 2400 X-ray fluorescent spectrometer and are available from the GSA Data Repository.[1] Rhenium and PGEs were determined by the isotopic dilution technique using spikes of ^{185}Re and a mixed spike of ^{105}Pd, ^{190}Os, ^{191}Ir, and ^{194}Pt. Rhenium was separated using anion resin after digestion of samples in HF-HNO_3. PGEs with spikes were concentrated into a Ni bead and dissolved in concentrated HNO_3. The analytical procedures are similar to those by Ravizza and Pyle (1997). Mass ratios were determined using an Elan 6000 ICP-MS from Perkin-Elmer Sciex. Typical blanks were 0.04–0.1 ng Re, 0.002–0.007 ng Ir/g flux, 0.002–0.006 ng Os/g flux, 0.07–16 ng Pt/g flux, and 0.03–0.9 ng Pd/g flux. The blanks are negligible compared to the amounts in the samples; thus blank corrections were not applied to the results. Mineral compositions were determined using a Cameca CAMEBAX SX100 microprobe with a counting time of 10 s/element, 20 kV accelerating potential, and 20 nA sample current. Standards used were albite (Si), MgO (Mg), Al_2O_3 (Al), Cr_2O_3 (Cr), Fe_2O_3 (Fe), $TiMnO_3$ (Ti, Mn), vanadinite (V), NiO (Ni), and Co metal (Co).

PETROGRAPHY AND GEOCHEMISTRY OF THE SERPENTINITES

All samples are intensely sheared and consist predominantly of antigorite and Cr spinel ± chrysotile. Sample CH52C is particularly rich in carbonates and chlorite. Two stages of serpentinization are recognized; the earlier is characterized by the crystallization of antigorite ± magnetite ± Mg-Ca carbonates and minor olivine and talc, and the later alteration formed chrysotile, chlorite, and carbonate veinlets at low temperatures. Spinel crystals in the Nidar and Zildat samples are 100–200 μm in diameter and are commonly rimmed by secondary magnetite (~50 μm wide). Chromite has relatively high Cr_2O_3 (48 to 58 wt%), with variable X_{Cr} (atomic ratio of Cr/[Cr + Al]) ranging from 0.56 to 0.84 (Fig. 2) and low TiO_2 (<0.2 wt%) and Fe_2O_3 (3–10 wt%). The Cr spinels from the Nidar ophiolite have the lowest X_{Cr} (~0.6), whereas those from the Zildat samples have higher X_{Cr} of ~0.8 due to lower Al_2O_3, <19.2 wt% (Fig. 2). The X_{Mg} values (atomic ratio Mg/[Mg+Fe^{2+}]) are similar (0.33–0.41) in all samples. A plot of X_{Cr} vs. X_{Mg} shows that the samples are similar to those of arc cumulates (Kepezhinskas et al., 1993; Arai, 1992), including those from southeast Alaskan complex (Bird and Clark, 1976) and the Jijal complex in Pakistan (Niida et al., 1998; Fig. 2). The chromite in our samples has a composition distinctly different from those in abyssal peridotites (shown as the oceanic mantle field in Fig. 2; Dick and Bullen, 1984). One of the Zildat samples (CH98b) contains olivine (~Fo_{96}) and talc in serpentine. The Mg content is higher than that of mantle olivines that are <Fo_{94} (e.g., Bonatti and Michael, 1989). Moreover, this olivine is not in equilibrium with the associated chromite (Arai, 1992). Considering the apparent equilibrium texture between the olivine and surrounding serpentine, we conclude that this olivine is a metamorphic product.

Bulk Chemical Composition

Most of our samples (Zildat samples and CH35a) contain high Cr (>2000 ppm), Ni (>2000 ppm), and MgO (>41 wt%), and low $Al2O_3$ (<1.0 wt%) and CaO (<1.0 wt%). The compositions are consistent with the original rocks being dunite or harzburgite from mantle residue (Ishii et al., 1992). In contrast, samples CH52C and TS18C contain low Ni and MgO, and high Al_2O_3 (9.4–19 wt%) and CaO (3.6–5.1 wt%), consistent with the occurrence of chlorite and relict plagioclase. Because Ca and Al are incompatible during partial melting, the data suggest their origin as crustal cumulates. Sample CH52C contains high Y (34 ppm) and Zr (81 ppm), values that are eight times those of primitive mantle. The data are consistent with the oceanic island origin of the Drakkarpo basalts (de Sigoyer, 1998).

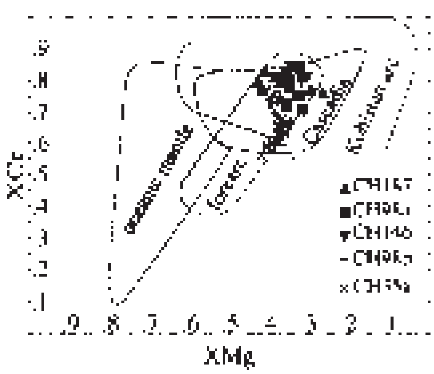

Figure 2. Composition of cores of chromian spinel; X_{Cr} = atomic ratio of Cr/(Cr + Al), X_{Mg}= atomic ratio of Mg/(Mg + Fe^{2+}). Note that spinel compositions are in field of those from subduction zones (forearc Kohistan arc, Cascadia samples in diagram) and that they are distinctly different from those from oceanic mantle. Data sources: oceanic mantle, Dick and Bullen (1984); Mariana forearc seamounts, Ishii et al. (1992); Cascadia zone, Bird and Clark (1976); Kohistan arc complex, Jan and Windley (1990).

Rhenium and PGEs

The contents of PGEs and Re show two patterns, samples with low Os and Ir (CH52C and TS18C) and the rest with overall high PGEs. The latter group shows flat, primitive mantle-normalized patterns with a depletion of Re and enrichment of Pd (Fig. 3). The moderate enrichment of Pd may be attributed to serpentinization because Pd is relatively mobile in saline fluids. The concentrations of PGEs and ratios of Pd/Ir and Pt/Ir are all similar to those of mantle nodules (e.g., Chou et al., 1983) and ultramafic massifs, such as Baldissero and Finero in the Ivrea zone and Ronda and Beni Bousera (Gueddari et al., 1996; Garuti et al., 1996). The PGE data therefore support a refractory mantle origin for the samples. Rhenium is incompatible during partial melting (e.g., Roy-Barman and Allegre, 1994), and the concentration of Re in melts is high even for those derived from a depleted mantle (Roy-Barman and Allegre, 1994). Thus the low Re suggests that these samples represent a mantle residue. The samples have high Os and Ir and low Al contents, and plot in the field of mantle residue (Fig. 4).

Samples TS18C and CH52 have low Os and Ir and high Pd and Pt (Fig. 3). Incompatible Re, Pt, and Pd may be enriched in magmas, whereas compatible Os and Ir remain in the mantle. Therefore, crustal rocks and even cumulates are generally low in Os and Ir. Examples include ultramafic cumulates of boninites at Heazelwoodite (Peck et al., 1992), dunite and wherlite of the Talkeetna arc in Alaska (Hattori and Hart, 1997), and the Kohistan arc in Pakistan (Hattori and Shirahase, 1997). Highly fractionated PGE patterns from TS18C and CH52C are consistent with a crustal cumulate origin for these two samples.

DISCUSSION

Origin of the Ladakh Serpentines

The mineral compositions, bulk compositions, and PGE concentrations of samples CH52C and

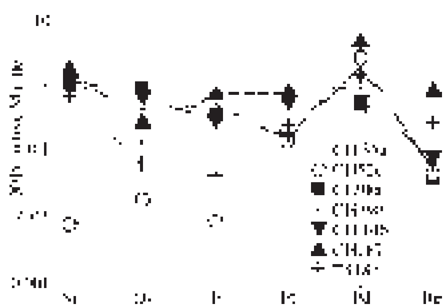

Figure 3. Primitive mantle-normalized plot of Ni, platinum group elements (PGE), and Re contents in serpentinites. Primitive mantle values are 1960 ppm for Ni and 0.28 ppb for Re (McDonough and Sun, 1995). Values for PGEs in primitive mantle are 0.00725 times of chondrite values of McDonough and Sun (1995): 3.55 ppb Os, 3.30 ppb Ir, 7.32 ppb Pt, and 3.99 ppb Pd. They are similar to measured concentration of mantle rocks by Chou et al. (1983) and Morgan (1986).

[1]GSA Data Repository item 200022, Table A, Bulk Chemical Composition of Serpentine Samples, and Table B, Olivine and Chromite Compositions, is available on request from Documents Secretary, GSA, P.O. Box 9140, Boulder, CO 80301-9140, editing@geosociety.org, or at www. geosociety.org/pubs/drpint.htm.

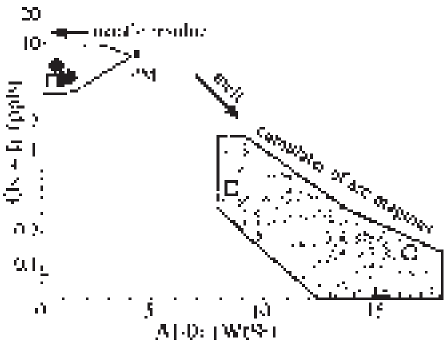

Figure 4. (Ir + Os) vs. Al_2O_3 of serpentinites (solid diamonds) compared to ultramafic cumulates of Jijal Complex in Pakistan and Talkeetna arc in Alaska (shaded area) and rocks of abyssal peridotite, Ronda and Beni Bousera massifs (shaded area). PM, primitive mantle data sources: Jijal complex, Hattori and Shirahase (1997); Talkeetna complex, Hattori and Hart (1997); Ronda and Beni Bosera massifs, Garuti et al. (1996); abyssal peridotites, Snow and Schmidt (1998). Serpentinite samples are plotted in field of refractory mantle residue, whereas data from samples TS18C and CH52C are similar to those of crustal cumulates.

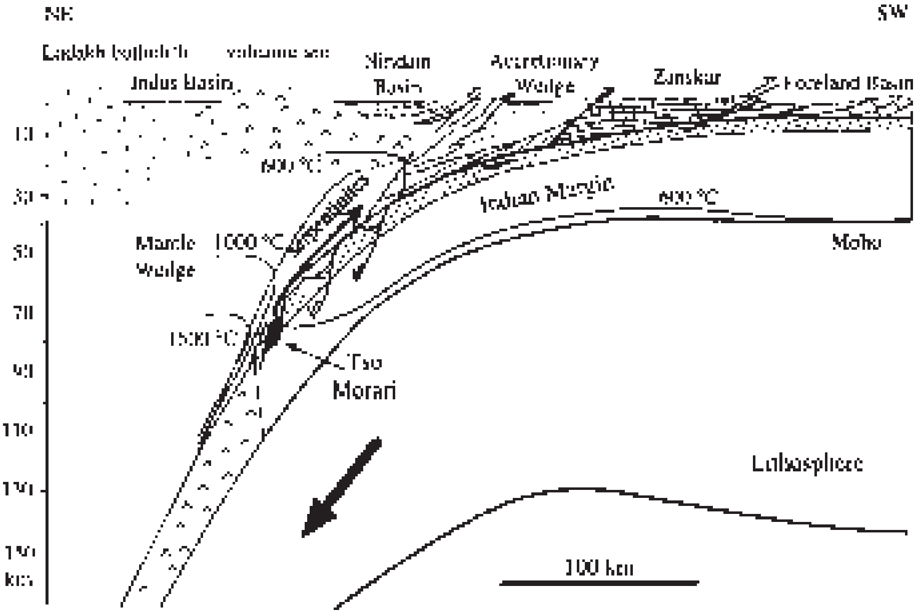

Figure 5. Schematic cross section of underplated Indian continental margin immediately prior to exhumation of Tso Morari eclogite unit at 50–55 Ma. Subduction of Tethyan oceanic crust was followed by underplating of Indian continental margin at 55 Ma. Earlier eclogitization in upper crust may cause upper crust to become stronger than lower crust, and may lead to decoupling of eclogitized crust and continued subduction of lower crust (Hacker, 1996). Detachment faults with horst-graben structures are common on margin of continent and it is likely that blocks of metamophosed rocks are isolated from rest of subducting slab. Such rigid blocks may be enclosed by ductile serpentinites and exhumed along subduction plane.

TS18C suggest that they are crustal cumulates. In contrast, the other serpentinite samples show strongly refractory characteristics in bulk composition, chromite chemistry, and PGE content. Chromite of similar composition may occur in cumulates of magmas, but the low Re and high Ir and Os contents rule out this possibility because ultramafic cumulates of arc magmas generally contain very little Os and Ir (Hattori and Hart, 1997; Hattori and Shirahase, 1997). Therefore, we conclude that the serpentinites represent samples from a hydrated mantle wedge. Low Al and Ca contents suggest at least 25%–35% previous melting (Ishiwatari, 1985).

The occurrence of metamorphic olivine in the Zildat samples suggests that serpentinization occurred at a relatively high temperature. The coexisting forsterite, talc, and antigorite without diopside and anthophyllite indicate metamorphic temperatures ranging from 500 to 650 °C (Mysen et al., 1998). In subduction zones, such temperatures are typically attained at depths between 50 and 70 km (Peacock, 1993). Therefore, serpentinization occurred under conditions similar to eclogitization (20 ± 2 kbar; 580 ± 50 °C) for the Tso Morari unit (Guillot et al., 1997). The transition from mafic blueschist to eclogite can occur at about 500 °C when the pressure exceeds 15 kbar in a subduction zone (Hacker, 1996). Such eclogitization is accompanied by the release of large amounts of water, which may cause hydration of the overlying mantle wedge (Peacock, 1993; Bebout and Barton, 1993). Focused fluid flow over a 40 km width would have lasted more than 10 m.y. at a subduction rate of 10 cm/yr (Peacock, 1993).

In the Himalaya, the Tethyan ocean crust of >4000 km length subducted until collision and underthrusting of the Indian continental margin occurred (Honegger et al., 1982). The overlying mantle wedge was probably serpentinized by dehydration of this oceanic crust and subsequent underthrusting of continental crust.

Evidence for Hydrated Mantle

In a subduction zone, it is expected that mantle peridotites are serpentinized due to dewatering of metasediments at depths of 5–20 km. These serpentinites may remain stable to depths of 200 km (Ulmer and Trommsdorf, 1995). The occurrence of hydrated mantle has been suggested from low seismic velocities in mantle wedges and reduced frictional stress along the subducting surface down to 70 km depth (Furukawa, 1993). This is further supported by high electrical conductivity along the tops of slabs (Wang et al., 1995).

Role of Serpentinite in the Exhumation of Ultrahigh-*P* and High-*P* rocks

The exhumation of metamorphic rocks requires a mechanically weak zone at the interface between the subduction plane and the rigid mantle wedge (Allemand and Lardeaux, 1997). At shallow depths, <40–50 km, hydrated sediments have a viscosity $<10^{17}$ Pa·s^{-1} (Cloos and Shreve, 1988) and can easily lubricate the interface between the two plates to facilitate exhumation of blocks of high-*P* rocks greater than hundreds of meters in size, as documented in the Franciscan Complex (Cloos and Schreve, 1988). At greater depths, >50 km, accretionary wedges pinch out, and sediment abundances decrease significantly. Serpentinites may replace the role of hydrated sediments at these greater depths and act as the lubricant for the exhumation of ultrahigh-*P* rocks. In addition, the geometry of accretionary wedges varies, and in some subduction zones, sediments may thin out at depths shallower than 50 km; in these situations, serpentinites may even contribute to the exhumation of high-*P* rocks.

Deformation experiments demonstrate that the strength of serpentinites decreases at temperatures between 400 and 600 °C at various pressures (Murrell and Ismail, 1976) and that the ductility increases as pressure increases above 400 MPa at room temperatures (Escartin et al., 1997). Moreover, hydration of peridotites reduces the shear stress at high pressures equivalent to >40 km depth (Strating and Vissers, 1991). This also causes a decrease in the viscosity, from 10^{26} Pa·s^{-1} to 10^{20} Pa·s^{-1} at 550 °C (Carter and Tsenn, 1987), and would assist upward movement of eclogites. Furthermore, the entire block composed of high-density eclogite (3200 kg·m^{-3}) and low-density serpentinite (2600 kg·m^{-3}) is buoyant compared to the surrounding dry peridotite (3200 kg·m^{-3}) and is likely to facilitate exhumation. Therefore, for these physical reasons, soft serpentinites between the subducting plate and the rigid mantle wedge at depths >40 km may commonly fulfill the role that sediments do at shallower depths (Fig. 5).

Our proposed model is consistent with the close association of ultrahigh-*P* rocks with serpentinites and hydrated peridotites in many active and former subduction zones (Table 1). Moreover, serpentinite likely played an important role in the exhumation of high-*P* rocks, considering their common occurrences in high-*P* metamorphic belts, such as the Catalina schist in California (Bebout and Barton, 1993), the Caribbean domain (e.g., Mann and Gordon, 1996), and the Sambagawa metamorphic belt (e.g., Kunugiza, 1984).

ACKNOWLEDGMENTS

This study was supported by the Centre National de la Recherche Scientifique and the Natural Sciences and Engineering Research Council of Canada. We thank Pascal Allemand, Gray E. Bebout, Ralph Kretz, Jean-Marc Lardeaux, Georgio Ranalli, and George Skippen for discussions and suggestions. Careful reviews and suggestions of Jane Selverstone and Bernard W. Evans were appreciated. We also thank Nicole Veschambre, Paul Capiez, Philippe Grandjean, Ron Hartree, and Monika Wilk for analytical assistance.

REFERENCES CITED

Allemand, P., and Lardeaux, J. M., 1997, Strain partitioning and metamorphism in a deformable orogenic wedge: Application to the Alpine belt: Tectonophysics, v. 280, p. 157–169.

Arai, S., 1992, Chemistry of chromian spinel in volcanic rocks as a potential guide to magma chemistry: Mineralogical Magazine, v. 56, p. 173–184.

Barnicoat, A. C., and Fry, N., 1986, High-pressure metamorphism of the Zermatt-Saas ophiolite, Switzerland: Geological Society of London Journal, v. 143, p. 607–618.

Bebout, G. E., and Barton, M. D., 1993, Metasomatism during subduction: Products and possible paths in the Catalina schists, California: Chemical Geology, v. 108, p. 61–92.

Bird, J. P., and Clark, A. L., 1976, Microprobe study of olivine chromitites of the Good News Bay ultramafic complex, Alaska, and the occurrence of platinum: U.S. Geological Survey Journal of Research, v. 4, p. 717–725.

Bonatti, E., and Michael, P. J., 1989, Mantle peridotites from continental rifts to ocean basins to subduction zones: Earth and Planetary Science Letters, v. 91, p. 297–311.

Carter, N., and Tsenn, M., 1987, Flow properties of continental lithosphere: Tectonophysics, v. 136, p. 27–63.

Chou, C. L., Shaw, D. M., and Crocket, J. H., 1983, Siderophile trace elements in the Earth's oceanic crust and upper mantle: Journal of Geophysical Research, v. 88, p. A507–A518.

Cloos, M., and Schreve, R. L., 1988, Subduction-channel model of prism accretion, melange formation, sediment subduction, and subduction erosion at convergent plate margins: Implications and discussion: Paleophysics, v. 128, p. 501–545.

de Sigoyer, J., 1998, Mécanismes d'exhumation des roches de haute pression haute temperature en contexte de convergence continentale [Ph.D. thesis]: Lyon, France, 200 p.

Dick, H. J. B., and Bullen, T., 1984, Chromian spinel as a petrogenetic indicator in abyssal and alpine-type peridotites and spatially associated lavas: Contributions to Mineralogy and Petrology, v. 86, p. 54–76.

Escartin, J., Hirth, G., and Evans, B., 1997, Nondilatant brittle deformation of serpentinites: Implications for Mohr-Coulomb theory and the strength of faults: Journal of Geophysical Research, v. 102, p. 2897–2913.

Furukawa, Y., 1993, Depth of the decoupling plate interface and thermal structure under arcs: Journal of Geophysical Research, v. 98, p. 20,005–20,013.

Garuti, G., Oddone, M., and Torres-Ruiz, J., 1996, Platinum-group element distribution in subcontinental mantle: Evidence from the Ivrea zone (Italy) and the Betic-Rifean cordillera (Spain and Morocco): Canadian Journal of Earth Sciences, v. 34, p. 444–463.

Gueddari, K., Piboule, M., and Amosse, J., 1996, Differentiation of platinum-group elements (PGEs) and of gold during partial melting of peridotites in the lherzolitic massif of the Betico-Rifean range (Ronda and Beni Bousera): Chemical Geology, v. 134, p. 181–197.

Guillot, S., de Sigoyer, J., Lardeaux, J. M., and Mascle, G., 1997, Eclogitic metasediments from the Tso Morari area (Ladakh, Himalaya): Evidence for continental subduction during India-Asia convergence: Contributions to Mineralogy and Petrology, v. 128, p. 197–212.

Hacker, B. R., 1996, Eclogite formation and the rheology, buoyancy, seismicity, and H_2O content of oceanic crust, *in* Bebout, G. E., et al., eds., Subduction top to bottom: American Geophysical Union Geophysical Monograph, 96, p. 337–346.

Hattori, K., and Hart, S. R., 1997, PGE and Os isotopic signatures for ultramafic rocks from the base of the Talkeetna island arc, Alaska: Eos (Transactions, American Geophysical Union), v. 78, p. 339.

Hattori, K., and Shirahase, T., 1997, Platinum group elements and osmium isotope signatures of the Kohistan island arc sequence, Himalaya-Karakaram area: Eos (Transactions, American Geophysical Union), v. 78, p. F-829.

Honegger, K., Dietrich, V., Frank, W., Gansser, A., Thoni, M., and Trommsdorff, V., 1982, Magmatism and metamorphism in the Ladakh Himalayas (the Indus-Tsangpo suture zone): Earth and Planetary Science Letters, v. 60, p. 253–292.

Ishii, T., Robinson, P. T., Maekawa, H., and Fiske, R., 1992, Petrological studies of peridotites from diapiric serpentinites seamounts in the Izu-Ogasawara-Mariana forearc, Leg 125: Scientific results, Volume 125: College Station, Texas, Ocean Drilling Program, p. 445–463.

Ishiwatari, A., 1985, Alpine ophiolites: Product of low-degree mantle melting in a Mesozoic transcurrent rift: Earth and Planetary Science Letters, v. 76, p. 93–108.

Jan, M. Q., and Windley, B. F., 1990, Chromian-spinel silicate chemistry in ultramafic rocks of the Jijal complex, northwest Pakistan: Journal of Petrology, v. 31, p. 667–715.

Kepezhinskas, P. K., Taylor, R. N., and Tanaka, H., 1993, Geochemistry of plutonic spinels from the north Kamchatka Arc: Comparisons with spinels from other tectonic settings: Mineralogical Magazine, v. 57, p. 575–589.

Kunugiza, K., 1984, Metamorphism and origin of ultramafic bodies of the Sanbagawa metamorphic belt in central Shikoku: Japanese Association of Mineralogists, Petrologists and Economic Geologists Journal, v. 75, p. 14–20.

Mann, P., and Gordon, M. K., 1996, Tectonic uplift and exhumation of blueschists belts along transpressional strike-slip fault zones, *in* Bebout, G. E., et al., eds., Subduction top to bottom: American Geophysical Union Geophysical Monograph, 96, p. 143–154.

Mayurama, S., Kaneko, Y., Terabayashi, M., Yamamoto, H., Nakajima, Y., Ota, T., Yamauchi, K., Katayama, I., and Ogasawara, Y., 1997, Geology of the Kokchetav UHP-HP unit, Northern Kazakhstan, *in* Ogasawara, Y., ed., Workshop on Kokchetav Deep-Drilling Project, Extended abstracts: Tokyo, Waseda University, p. 3–8.

McDonough, W., and Sun, S. S., 1995, The composition of the earth: Chemical Geology, v. 120, p. 223–253.

Medaris, L. G., and Carswell, D. A., 1989, Petrogenesis of Mg-Cr garnet peridotites in European metamorphic belts, *in* Carswell, D. A., ed., Eclogite facies rocks: London, Blackie and Son Ltd., p. 260–290.

Morgan, J. W., 1986, Ultramafic xenoliths: Clues to earth's late accretionary history: Journal of Geophysical Research, v. 91, p. 12,375–12,387.

Murrell, S. A. F., and Ismail, I. A. H., 1976, The effect of decomposition of hydrous minerals on the mechanical properties of rocks at high pressure and temperatures: Tectonophysics, v. 31, p. 207–258.

Mysen, B., Ulmer, P., Konzett, J., and Schmidt, M. W., 1998, The upper mantle near convergent plate boundaries, *in* Hemley, R. J., ed., Ultrahigh-pressure mineralogy: Mineralogical Society of America, Reviews in Mineralogy, v. 37, p. 97–138.

Niida, Y., Terai, Y., Rahim Khan, S., and Kausar, A. B., 1998, Origin of chromitites from the Jijal complex, Kohistan arc, north Pakistan, *in* Sobel, E., et al., eds., 13th Himalaya-Karakoram-Tibet International Workshop: Peshawar, Terra Nostra, Schriften der Alfred-Wegener-Stiftung 99/2, p. 140–141.

Parkinson, C. D., Miyazaki, K., Wakita, K., Barber, A. J., and Carswell, D. A., 1997, Very high-pressure metamorphic and associated rocks of Java, Sulawesi and Kalimantan, Indonesia, *in* Ogasawara, Y., ed., Workshop on Kokchetav Deep-Drilling Project, Extended abstracts: Tokyo, Waseda University, p. 140–141.

Peacock, S. M., 1993, Metamorphism, dehydration, and importance of the blueschist-eclogite transition in subducting oceanic crust: Geological Society of America Bulletin, v. 105, p. 684–694.

Peck, D. C., Keays, R. R., and Ford, R. J., 1992, Direct crystallization of refractory platinum-group element alloys from boninitic magmas; evidence from western Tasmania: Australian Journal of Earth Sciences, v. 39, p. 373–387.

Platt, J. P., 1993, Exhumation of high-pressure metamorphic rocks: A review of concepts and processes: Terra Nova, v. 5, p. 119–133.

Ravizza, G., and Pyle, D., 1997, PGEs and Os isotopic analyses of single sample aliquots with NiS fire assay preconcentration: Chemical Geology, v. 141, p. 251–268.

Roy-Barman, M., and Allegre, C. J., 1994, $^{187}Os/^{186}Os$ ratios of mid-ocean ridge basalts and abyssal peridotites: Geochimica et Cosmochimica Acta, v. 58, p. 5043–5054.

Scamberulli, M., Muntener, O., Hermann, J., Piccardo, G. B., and Trommsdorff, V., 1995, Subduction of water into the mantle: History of an alpine peridotite: Geology, v. 23, p. 459–462.

Schmädicke, E., Okrusch, M., and Schmidt, W., 1992, Eclogite-facies rocks in the Saxonian Erzerbirge, Germany: HP metamorphism under contrasting *P-T* conditions: Contributions to Mineralogy and Petrology, v. 110, p. 226–241.

Snow, J. E., and Schmidt, G., 1998, Constraints on Earth accretion deduced from noble metals in the oceanic mantle: Nature, v. 391, p. 167–169.

Strating, E. H. H., and Vissers, R. L. M., 1991, Dehydration-induced fracturing of eclogite-facies peridotites: Implications for the mechanical behaviour of subducting oceanic lithosphere: Tectonophysics, v. 200, p. 187–198.

Ulmer, P., and Trommsdorff, V., 1995, Serpentinite stability to mantle depths and subduction related magmatism: Science, v. 268, p. 858–861.

Wang, K., Mulder, T., Rogers, C., and Hyndman, R. D., 1995, Case for very low coupling stress on the Cascadia subduction fault: Journal of Geophysical Research, v. 100, p. 12,907–12,918.

Zhang, Y. Q., and Liou, J. G., 1994, Petrogenesis of garnet-bearing ultramafic rocks and associated eclogites in the Sulu ultrahigh pressure metamorphic terrane, China: Journal of Metamorphic Geology, v. 12, p. 169–186.

Manuscript received July 12, 1999
Revised manuscript received November 1, 1999
Manuscript accepted November 9, 1999

TABLE A. BULK CHEMICAL COMPOSITION OF SERPENTINE SAMPLES *

Sample	CH35a	CH52c	CH98a	CH98b	CH146	CH187	TS18c
SiO_2 (wt.%)	38.68	29.55	35.05	40.15	40.59	39.39	38.09
TiO_2	0.02	0.374	0.03	0.015	0.024	0.023	0.032
Al_20_3	0.49	16.72	0.54	0.37	0.77	1.09	8.44
Fe_20_3 (t)**	7.58	5.55	6.83	7.54	7.59	8.99	8.19
Mn0	0.1	0.277	0.127	0.1	0.093	0.105	0.107
Mg0	38.56	29.65	39.97	41.82	36.65	38	30.59
CaO	0.65	4.41	0.64	0.29	1.05	0.33	3.22
Na_2O	<0.005	<0.005	<0.005	<0.005	<0.005	<0.005	0.16
K_2O	<0.005	<0.005	<0.005	<0.005	<0.005	<0.005	0.005
P_20_5	0.004	0.081	0.005	0.006	0.004	<0.001	0.003
LOI***	13.8	14.7	17	9.8	13.1	11.8	11.1
Cr (ppm)	2121	32	2718	2604	2581	2778	3159
V	28	48	19	18	34	37	27
Co	107	<10	97	110	93	113	94
Zn	49	21	51	54	30	32	45
Ni	2222	16	2255	2825	2260	2393	1387
Ga	<10	13	<10	<10	<10	<10	<10
Zr	<5	69	<5	<5	<5	<5	<5
Y	<5	29	<5	<5	<5	<5	<5
Sr	10	28	24	12	17	5	36
Pb	140	<10	450	111	<15	315	15
Th	<10	<10	14	<10	<10	11	<10
U	<10	<10	30	<10	<10	17	<10
Os (ppb)	2.2	0.08	3.77	1.4	3.0	1.6	0.27
Ir	2.25	0.041	1.53	2.95	1.39	2.83	0.187
Pt	2.1	1.2285	1.4635	6.8075	5.0735	5.467	2.03
Pd	8.36	11.8	2.23	4.69	2.84	20.1	5.82
Re	0.013	0.013	0.012	0.020	0.027	0.20	0.078
Total (wt.%)	100.33	101.32	100.70	100.65	100.36	100.26	100.40

* The concentration of major and minor elements was determined on fused disks using a Philips PW-2400 X-ray fluorescent spectrometer in Ottawa.

** Fe total is expressed as Fe_2O_3

The contents of Rb Nb La, Ce, Nd and Ba are below detection limits,< 5 ppm for Rb and Nb and 50 ppm for the rest of elements.

*** Loss of ignition, determined after heating samples for >1hr at 1050 C

TABLE B. OLIVINE AND CHROMITE COMPOSITIONS

Mineral	Olivine	Olivine		chromite	chromite	chromite	chromite	chromite
Sample	CH98b	CH98b		CH35a	CH98a	CH98b	CH146	CH187
SiO2	42.73	42.67	SIO2	0.03	0.02	0.00	0.00	0.04
TiO2	0.04	0.04	TiO2	0.10	0.04	0.04	0.19	0.07
FeO	3.95	3.81	Al2O3	18.80	8.82	9.29	6.66	9.82
Cr2O3	0.00	0.00	Cr2O3	42.67	57.07	58.74	53.49	55.90
MgO	54.83	54.78	Fe2O3	7.33	3.82	2.92	9.94	4.48
MnO	0.25	0.16	FeO	27.45	22.90	21.70	23.00	21.98
NiO	0.00	0.00	MgO	7.88	6.74	7.72	6.30	7.42
CaO	0.02	0.03	MnO	0.68	0.00	0.00	0.00	0.00
NiO	0.00	0.00	NiO	0.09	0.03	0.05	0.05	0.00
			ZnO	0.02	0.00	0.16	0.29	0.21
Total	101.82	101.48	total	100.25	99.64	100.84	100.13	100.40
Calc. based on 4 O			Calc. based on 32 O					
Si	1.00	1.00	Si	0.00	0.00	0.00	0.00	0.01
Ti	0.00	0.00	Ti	0.00	0.01	0.01	0.04	0.01
Fe	0.08	0.07	Al	5.77	2.85	2.94	2.17	3.13
Mg	1.91	1.92	Cr	8.78	12.36	12.46	11.71	11.95
Mn	0.00	0.00	Fe3+	1.44	0.79	0.59	2.07	0.91
Ni	0.00	0.00	Fe2+	4.77	5.24	4.87	5.33	4.97
Al	0.00	0.00	Mg2+	3.06	2.75	3.09	2.60	2.99
Ca	0.00	0.00	Mn2+	0.15	0.00	0.00	0.00	0.00
Total	3.00	3.00	Ni2+	0.02	0.01	0.01	0.01	0.00
			Zn2+	0.00	0.00	0.03	0.06	0.04
% Fo	96.11	96.25						
			Cr#	0.60	0.81	0.81	0.84	0.79
			Mg#	0.39	0.34	0.39	0.33	0.38